J|A|C|S
ARTICLES
Published on Web 01/04/2003

Molecular Dynamics and Quantum Chemical Studies on the Catalytic Mechanism of Δ^5-3-Ketosteroid Isomerase: The Catalytic Diad versus the Cooperative Hydrogen Bond Mechanism

Hwangseo Park and Kenneth M. Merz, Jr.*

Contribution from the 152 Davey Laboratory, Department of Chemistry, Pennsylvania State University, University Park, Pennsylvania 16802-6300

Received June 7, 2002; E-mail: merz@psu.edu

Abstract: To further understand Δ^5-3-ketosteroid isomerase (KSI) catalysis, we carried out molecular dynamics (MD) simulations of the KSI dimer ligated with a substrate and reaction intermediate analogue and high level ab initio calculations on relevant enzymatic reaction models. Simulation of the enzyme−substrate complex dimer systems showed asymmetric dynamics between the two monomers, in which the hydrogen bond pattern between the substrate and active site residues in the first and the second subunits supported the cooperative hydrogen bond (CH) and the catalytic diad (CD) mechanisms, respectively. On the other hand, only the CH mechanism was supported in the MD simulation of the enzyme−intermediate complex dimer. From MP2/6-31+G**//RHF/6-31G** calculations, we found the kinetic barriers for the two reaction mechanisms were similar. The CH route afforded a greater stabilization to the enolate intermediate than did the CD counterpart. Thus, the present computational studies indicate that the CH mechanism would be favored over the CD one in the catalytic action of KSI. However, the latter could not be ruled out conclusively because of the explicit appearance of a CD configuration in the MD trajectories of the enzyme−substrate complex and because of the similar intrinsic activation barrier for the CH and CD mechanisms. The appearance of configurations that favor the CD pathway is rationalized in terms of a model in which the KSI−substrate complex does not have a strong preference for one hydrogen bonding pattern over another, while the KSI−intermediate complex favors a cooperative hydrogen bond pattern in order to stabilize the reaction intermediate. This hypothesis is supported by the ab initio calculations which indicate that the CH intermediate is more stable than the CD one by ~6.3 kcal/mol.

1. Introduction

Δ^5-3-Ketosteroid isomerase (KSI) is one of the most proficient enzymes known. KSI catalyzes the isomerization reaction of Δ^5- to Δ^4-3-ketosteroids at a rate that approaches the diffusion-controlled limit.[1] The three-dimensional structures of KSIs from two bacterial strains, *Pseudomonas testosteroni* and *Pseudomonas putida* Biotype B, have been obtained by NMR and X-ray crystallography.[2] Despite having only 34% sequence identity, the two KSIs are believed to have common catalytic mechanisms due to the conservation of major catalytic residues and the close similarity of the 3D structures.

It is generally agreed that the catalytic reaction proceeds through the formation of a dienolate intermediate formed by the cleavage of a C−H bond adjacent to the substrate carbonyl group and a subsequent reketonization step. In an effort to understand the overall catalytic strategy for an highly efficient combination of enolization/reketonization, the detailed catalytic mechanism of related enzymes such as triose-phosphate isomerase,[3] mandelate racemase,[4] citrate synthase,[5] and so forth have also been examined.

Early crystallographic and mechanistic studies on KSI suggested that Tyr14 and Asp38 were essential catalytic residues, acting as a general acid catalyst and a proton shuttle, respectively.[6] However, the involvement of an additional acid residue

* To whom correspondence should be addressed. Fax: +1-814-863-8403.

(1) Radzicka, A.; Wolfenden, R. *Science* **1995**, *267*, 90.
(2) (a) Wu, Z. R.; Ebrahimian, S.; Zawrotny, M. E.; Thornburg, L. D.; Perez-Alvarado, G. C.; Brothers, P.; Pollack, R. M.; Summers, M. F. *Science* **1997**, *276*, 415. (b) Kim, S. W.; Cha, S. S.; Cho, H. S.; Kim, J. S.; Ha, N. C.; Cho, M. J.; Joo, S.; Kim, K. K.; Choi, K. Y.; Oh, B. H. *Biochemistry* **1997**, *36*, 14030. (c) Ha, N. C.; Kim, M. S.; Lee, W.; Choi, K. Y.; Oh, B. H. *J. Biol. Chem.* **2000**, *275*, 41100.
(3) (a) Gerlt, J. A.; Gaussman, P. G. *Biochemistry* **1993**, *32*, 11934. (b) Lodi, P. J.; Knowles, J. R. *Biochemistry* **1991**, *30*, 6948. (c) Shan, S.; Herschlag, D. *Proc. Natl. Acad. Sci. U.S.A.* **1996**, *93*, 14474. (d) Lennartz, C.; Schafer, A.; Terstegen, F.; Thiel, W. *J. Phys. Chem. B* **2002**, *106*, 1758. (e) Cui, Q.; Karplus, M. *J. Phys. Chem. B* **2002**, *106*, 1768.
(4) Landro, J. A.; Gerlt, J. A.; Kozarich, J. W.; Koo, C. W.; Shah, V. J.; Kenyon, G. L.; Neidhart, D. J.; Fujita, J. R.; Clifton, J. R.; Petsko, G. A. *Biochemistry* **1994**, *33*, 635. (b) Mitra, B.; Kalarakal, A. T.; Kozarich, J. W.; Gerlt, J. A.; Clifton, J. R.; Petsko, G. A.; Kenyon, G. L. *Biochemistry* **1995**, *34*, 2777. (c) Larson, T. M.; Wedekind, J. E.; Rayment, I.; Reed, G. H. *Biochemistry* **1996**, *35*, 4349.
(5) (a) Remington, S. J. *Curr. Opin. Struct. Biol.* **1992**, *2*, 730. (b) Usher, K. C.; Remington, S. J.; Martin, D. P.; Drueckhammer, D. G. *Biochemistry* **1994**, *33*, 7753.
(6) (a) Kuliopulos, A.; Mildvan, A. S.; Shortle, D.; Talalay, P. *Biochemistry* **1989**, *28*, 149. (b) Bounds, P. L.; Pollack, R. M. *Biochemistry* **1987**, *26*, 2263. (c) Zawrotny, M. E.; Hawkinson, D. C.; Blotny, G.; Pollack, R. M. *Biochemistry* **1996**, *35*, 6438. (d) Viger, A.; Coustal, S.; Marquet, A. *J. Am. Chem. Soc.* **1981**, *103*, 451. (e) Xie, L.; Talalay, P.; Mildvan, A. S. *Biochemistry* **1991**, *30*, 10858.

Scheme 1

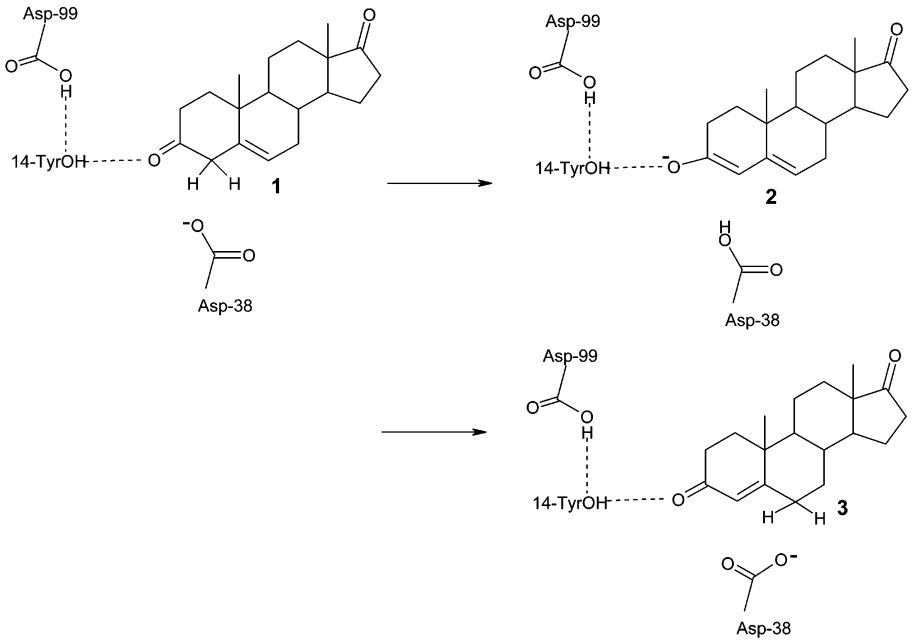

in the catalytic action of KSI was also suspected from several lines of experimental evidence without it ever being unambiguously proven.[7] Recent structural analyses by multidimensional heteronuclear NMR spectroscopy and X-ray crystallography showed that an acid residue, namely Asp99, also participates in the enzymatic reaction as an additional electrophilic catalyst, playing a significant role in the stabilization of the negative charge developed on the substrate carbonyl oxygen during the catalytic cycle.[2a,b] From site-directed mutagenesis studies, it was reported that the contribution of Asp99 to enzymatic catalysis is a little smaller than that of Tyr14.[8]

Despite these new findings, the nature of catalysis by Asp99 in the enzymatic reaction is still a matter of much debate. In this regard, two possibilities have been suggested on the basis of available experimental evidence. The first, in what is called the catalytic diad (CD) mechanism, involves a strong hydrogen bond between the carboxylate group of Asp99 and the phenolic oxygen of Tyr14 (Scheme 1). This interaction increases the electrophilicity of Tyr14, thereby promoting its ability to donate a hydrogen bond to the carbonyl oxygen of the ketosteroid substrate. The formation of the CD was proposed on the basis of NMR detection of highly deshielded resonance peaks and their disappearance in mutants lacking Tyr14.[9] Further evidence for this mechanism came from the solution structure of the enzyme complexed with a substrate analogue.[10]

The second alternative, the cooperative hydrogen bond (CH) mechanism, differs from the CD route in that both Tyr14 and Asp99 participate in catalysis by forming direct hydrogen bonds with the steroid carbonyl oxygen (Scheme 2). After the first mechanistic proposal,[2a] new experimental evidence suggests that there is a direct interaction between Asp99 and the substrate carbonyl oxygen.[11] Furthermore, it has also been argued that the highly deshielded ^{1}H NMR peaks can be observed even if the catalytic diad formation is ruled out.[11b] Hence, current thinking favors the CH route, although the CD cannot be conclusively eliminated.

Although most previous mechanistic studies were performed with experimental tools such as X-ray crystallography, multidimensional heteronuclear NMR, mutagenesis, and kinetic measurements, some ab initio results have also been reported at varying levels of theory. On model systems for the CH mechanism, Kim and co-workers provided computational support for the experimentally proposed structural features and the effect of mutations on KSI catalysis.[12] Pan and McAllister estimated the relative stability of model reaction intermediates formed during the two possible reaction mechanisms.[13] Although the role of Asp38 in the catalytic reaction was not considered explicitly, they provided evidence that the reaction intermediates were stabilized to a similar extent in both of the possible mechanisms.

The present work was undertaken to address the detailed role of Asp99 on the enzymatic reaction on the basis of MD simulations of the KSI dimers complexed with the substrate analogue, 19-nortestosterone hemisuccinate (19-NTH), and the reaction intermediate analogue, equilenin (EQU; see Figure 1). During the MD simulations, we monitored the relative position

(7) (a) Austin, J. C.; Kuliopulos, A.; Mildvan, A. S.; Spiro, T. G. *Protein Sci.* **1992**, *1*, 259. (b) Austin, J. C.; Zhao, Q.; Jordan, T.; Talalay, P.; Mildvan, A. S.; Spiro, T. G. *Biochemistry* **1995**, *34*, 4441. (c) Li, Y.-K.; Kuliopulos, A.; Mildvan, A. S.; Talalay, P. *Biochemistry* **1993**, *32*, 1816. (d) Holman, C. M.; Benisek, W. F. *Biochemistry* **1995**, *34*, 14245. (e) Weintraub, H.; Alfsen, A.; Baulieu, E.-E. *Eur. J. Biochem.* **1970**, *12*, 217.

(8) Choi, G.; Ha, N. C.; Kim, S. W.; Kim, D. H.; Park, S.; Oh, B. H.; Choi, K. Y. *Biochemistry* **2000**, *39*, 903.

(9) (a) Zhao, Q.; Abeygunawardana, C.; Talalay, P.; Mildvan, A. S. *Proc. Natl. Acad. Sci. U.S.A.* **1996**, *93*, 8220. (b) Zhao, Q.; Abeygunawardana, C.; Gittis, A. G.; Mildvan, A. S. *Biochemistry* **1997**, *36*, 14616.

(10) Massiah, M. A.; Abeygunawardana, C.; Gittis, A. G.; Mildvan, A. S. *Biochemistry* **1998**, *37*, 14701.

(11) (a) Thornburg, L. D.; Henot, F.; Bash, D. P.; Hawkinson, D. C.; Bartel, S. D.; Pollack, R. M. *Biochemistry* **1998**, *37*, 10499. (b) Pollack, R. M.; Thornburg, L. D.; Wu, Z. R.; Summers, M. F. *Arch. Biochem. Biophys.* **1999**, *370*, 9. (c) Cho, H. S.; Choi, G.; Choi, K. Y.; Oh, Y. H. *Biochemistry* **1998**, *37*, 8325. (d) Kim, D. H.; Jang, D. S.; Nam, G. H.; Choi, G.; Kim, J. S.; Ha, N. C.; Kim, M. S.; Oh, B. H.; Choi, K. Y. *Biochemistry* **2000**, *39*, 4581. (e) Cho, H. S.; Ha, N. C.; Choi, G.; Kim, H. J.; Lee, D.; Oh, K. S.; Kim, K. S.; Lee, W.; Choi, K. Y.; Oh, B. H. *J. Biol. Chem.* **1999**, *274*, 32863−32868.

(12) (a) Kim, K. S.; Oh, K. S.; Lee, J. Y. *Proc. Natl. Acad. Sci. U.S.A.* **2000**, *97*, 6373. (b) Oh, K. S.; Cha, S. S.; Kim, D. H.; Cho, H. S.; Ha, N. C.; Choi, G.; Lee, J. Y.; Tarakeshwar, P.; Son, H. S.; Choi, K. Y.; Oh, B. H.; Kim, K. S. *Biochemistry* **2000**, *39*, 13891−13896.

(13) Pan, Y.; McAllister, M. A. *THEOCHEM* **2000**, *504*, 29.

Scheme 2

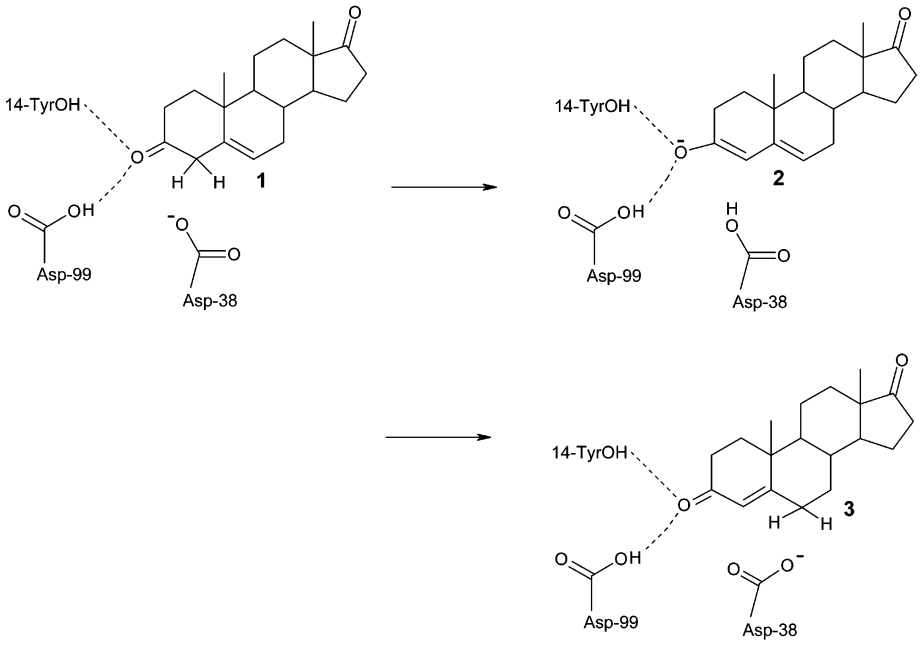

of Asp99 with respect to Tyr14 and the substrate carbonyl oxygen and phenolic oxygen of EQU in both subunits of the homodimeric system in order to obtain insights into the specific orientations of these groups and how they might affect catalysis.

To complement the solution phase all-atom MD simulation studies, we carried out high level ab initio calculations on simplified model systems to estimate the free energy profiles associated with the two catalytic reaction pathways. Shown in Scheme 3 are the enzymatic reaction models for the CD and the CH mechanisms under investigation.

In these model systems, 3-butenal, the simplest β,γ-unsaturated carbonyl compound, mimics the substrate, while formate, phenol, and formic acid were used to model the side chains of Asp38, Tyr14, and Asp99 in the active site of KSI, respectively. By determining the free energy profile and stationary-state structures along the intrinsic reaction coordinates (IRC) of the two model enzymatic reactions, we will address the kinetic and thermodynamic aspects of the catalytic mechanisms.

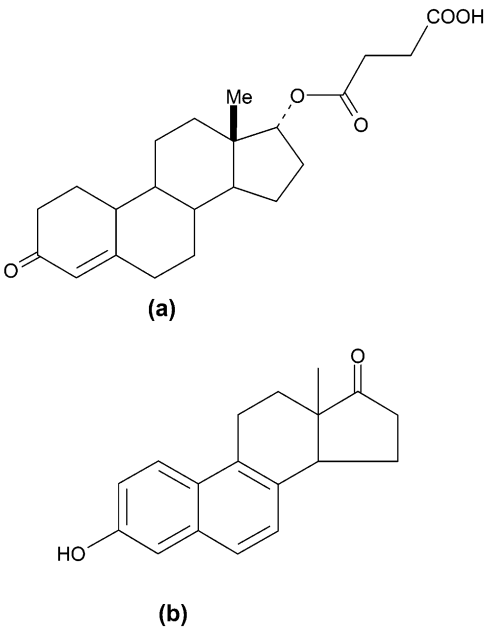

Figure 1. Molecular structures of (a) 19-nortestosterone hemisuccinate (19-NTH) and (b) equilenin (EQU).

2. Computational Methods

MD simulations of the KSI dimers from *P. testosteroni*, where both monomers were complexed with 19-NTH or EQU, were carried out using the SANDER module of AMBER 6[14] with the force field reported by Cornell et al.[15] As a starting coordinate, we chose the lowest energy conformer of 15 reported NMR structures of KSI ligated with 19-NTH in which Asp38 is ionized and Asp99 is protonated.[10] In the case of the KSI−EQU complex system, the X-ray crystal structure was used.[11e] Atomic charges for 19-NTH and EQU were calculated with the Merz−Kollman/Singh method[16] for fitting point charges to the quantum mechanical electrostatic potential calculated at the RHF/6-31G* level. Missing force field parameters were estimated from similar chemical constructs contained within the AMBER force field database. The all-atom models were neutralized by adding sodium ions and were immersed in a rectangular box containing about 10 thousands TIP3P water molecules. After 2000 cycles of energy minimization to remove bad van der Waals contacts, we equilibrated the system beginning with 20 ps of equilibration of the solvent molecules at 298 K. The next step involved equilibration of the solute with a fixed configuration for the solvent molecules for 5 ps at 10, 50, 100, 150, 200, 250, and finally 298 K. Then, the initial equilibration dynamics of the entire system was performed at 298 K for 20 ps. Following the initial equilibration, a 600 ps MD simulation was carried out with periodic boundary conditions in the NPT ensemble at 298 K using the Berendsen temperature coupling[17] and constant pressure (1 atm) with isotropic molecule-based scaling. The SHAKE algorithm,[18] with a tolerance of

(14) Case, D. A.; Pearlman, D. A.; Caldwell, J. W.; Cheatham, T. E., III.; Ross, W. S.; Simmerling, C.; Darden, T.; Merz, K. M., Jr.; Stanton, R. V.; Chen, A.; Vincent, J. J.; Crowley, M.; Tsui, V.; Radmer, R.; Duan, Y.; Pitera, J.; Massova, I.; Seibel, G. L.; Singh, U. C.; Weiner, P.; Kollman, P. A. *AMBER 6*; University of California, San Francisco: San Francisco, CA, 1999.
(15) Cornell, W. D.; Cieplak, P.; Bayly, C. I.; Gould, I. R.; Merz, K. M., Jr.; Ferguson, D. M.; Spellmeyer, D. C.; Fox, T.; Caldwell, J. W.; Kollman, P. A. *J. Am. Chem. Soc.* **1995**, *117*, 5179.
(16) Besler, B. H.; Merz, K. M., Jr.; Kollman, P. A. *J. Comput. Chem.* **1990**, *11*, 431.
(17) Berendsen, H. C.; Postma, J. P. M.; van Gunsteren, W. F.; DiNola, A.; Haak, J. R. *J. Comput. Phys.* **1984**, *81*, 3684
(18) Ryckaert, J. P.; Ciccotti, G.; Berendsen, H. C. *J. Comput. Phys.* **1977**, *23*, 327.

Scheme 3

A. Catalytic Diad Mechanism

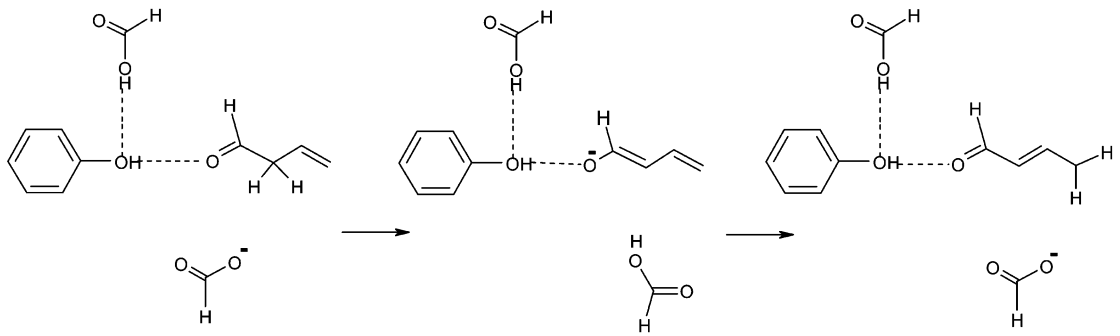

B. Cooperative Hydrogen Bond Mechanism

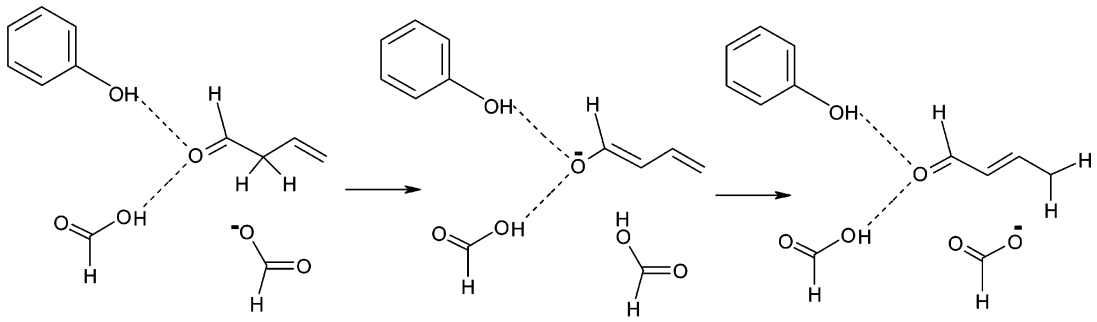

10^{-6}, was applied to fix all bond lengths involving a hydrogen atom. We used a time step of 1 fs and a nonbond cutoff of 10 Å; the trajectory was sampled every 0.1 ps (100 step intervals).

All structures corresponding to minima and transition states on the two model enzymatic reaction pathways were optimized at the RHF/6-31G** level of theory with GAMESS.[19] No structural restraints were used in the ab initio geometry optimizations to ensure that the final structures should be a true energy minimum or a saddle point on the potential energy surface. However, to maintain the original structures as much as possible, we used a very small trust radius of 0.1 Bohr in optimizing the geometry of **CDR** and **CHR** starting from the NMR and X-ray structures, respectively. The geometry optimizations were performed using analytically determined gradients and quasi-Newton−Raphson optimization algorithms.[20] The nature of each SCF stationary point was determined by the number of imaginary frequencies that were obtained by diagonalizing the analytical Hessian matrix. Each transition state structure was determined to have a single negative eigenvalue, and the corresponding imaginary vibrational frequency was related to the motion that would connect the expected starting and final minima. The intrinsic reaction coordinate (IRC) connecting a transition state to the neighboring energy minima was determined using the Gonzalez−Schlegel second-order (GS2) method[21] at the same level of theory as the geometry optimizations.

To get a better prediction for the energetics, we performed post-HF level calculations including the effect of electron correlation at the optimized geometries. These single point calculations were carried out with the 6-31+G** basis sets using Møller−Plesset second-order perturbation theory (MP2).[22] The electronic energies computed in this way were used to calculate the relative free energies (ΔG) that are given by

$$\Delta G = \Delta E_{\text{elec}} + \Delta H' - T\Delta S \quad (1)$$

Here, $\Delta H'$ denotes the enthalpy change due to thermal motions of the nuclei including the zero-point vibrational energies, and ΔS is the entropy change. While the electronic energies (E_{elec}) were evaluated using MP2/6-31+G** level calculations, the vibrational frequencies used to estimate $\Delta H'$ and ΔS were obtained at the RHF/6-31G** level.

3. Results and Discussion

3.1. MD Simulation of KSI Dimer in Complex with 19-NTH. As a measure of structural stability, root-mean-square deviations from the NMR structure (rmsd_{NMR}) were calculated on the basis of a superposition of all protein and ligand atoms. The values were obtained by independent fits of each monomer to the solution phase NMR structure to eliminate the contribution of relative subunit motions. As seen in Figure 2, the rmsd_{NMR} values are between 2.0 Å and 2.9 Å throughout the simulation time, indicating that neither subunit of the protein−ligand complex has undergone a substantial structural change during the simulation. Interestingly, however, the rmsd_{NMR} of subunit A is found to be greater than that of subunit B for a large part of the simulation time, although the difference remains within 0.6 Å. This suggests that the two enzyme−substrate complex subunits are exploring different regions of configuration space. As might be expected, a similar pattern is found for the rmsd_{NMR} for each residue from their NMR structure positions (Figure 3).

Figure 4 displays the variation of the interatomic distances between the phenolic hydrogen (HH) of the Tyr14 side chain and substrate carbonyl oxygen (O_S) during the unconstrained

(19) Schmidt, M. W.; Baldridge, K. K.; Boatz, J. A.; Elbert, S. T.; Gordon, M. S.; Jensen, J. H.; Koseki, S.; Matsunaga, N.; Nguyen, K. A.; Su, S.; Windus, T. L.; Dupuis, M.; Montgomery, J. A. *J. Comput. Chem.* **1993**, *14*, 1347.
(20) (a) Baker, J. *J. Comput. Chem.* **1986**, *7*, 385. (b) Helgaker, T. *Chem. Phys. Lett.* **1991**, *182*, 305. (c) Bell, S.; Crighton, J. S. *J. Chem. Phys.* **1984**, *80*, 2464.
(21) Gonzalez, C.; Schlegel, B. H. *J. Chem. Phys.* **1989**, *90*, 2154.
(22) Møller, C.; Plesset, M. S. *Phys. Rev.* **1934**, *46*, 618.

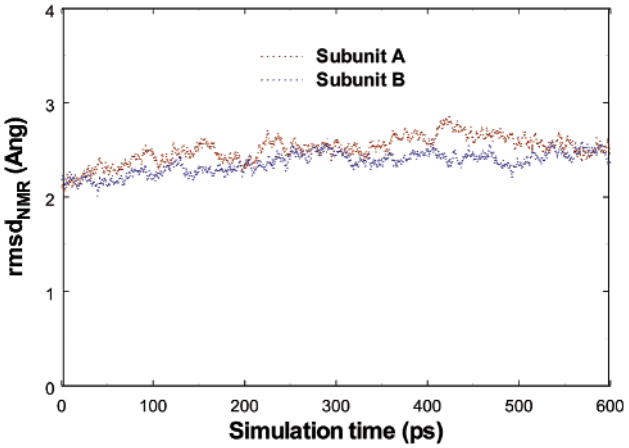

Figure 2. Time dependence of the root-mean-square deviation from the NMR structure (rmsd$_{NMR}$) for subunit A and B of the KSI−19-NTH complex dimer. Each monomer was separately fitted to the NMR structure in calculating the rmsd$_{NMR}$ values.

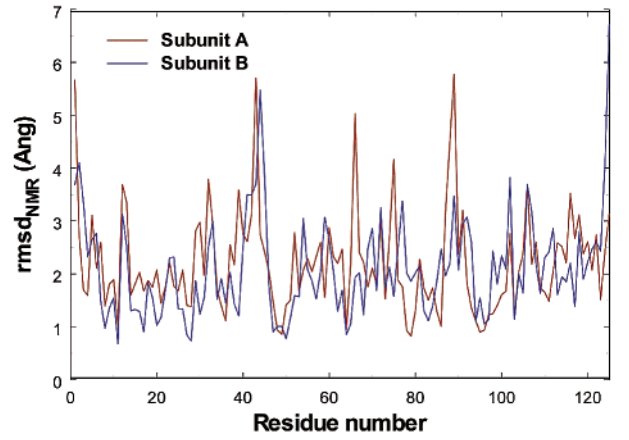

Figure 3. Root-mean-square deviations of each residue from the NMR structure averaged over the 600 ps MD simulation.

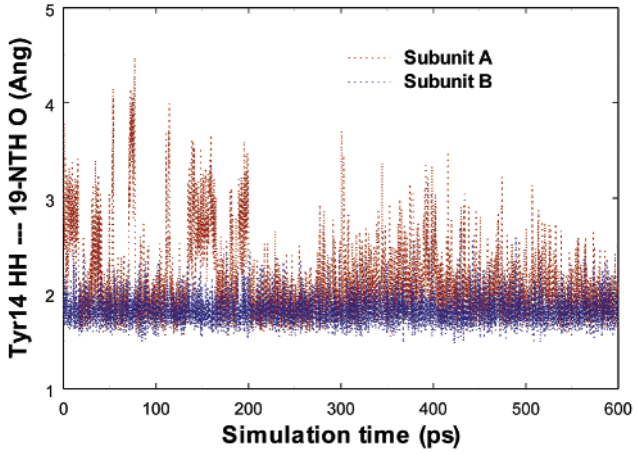

Figure 4. Maintenance of the hydrogen bonding distance between the substrate carbonyl oxygen and HH atom of Tyr14 in both monomers of the enzyme−19-NTH complex dimer. Mean values of the distances in subunit A and subunit B are 2.12 and 1.83 Å, respectively.

MD simulation. In the protein−19-NTH complex dimer, the distance is maintained at ∼2.5 Å for 85% and 100% of simulation time in subunit A and B, respectively. This interaction, observed in both subunits, is consistent with the common structural feature of the two competing catalytic mechanisms: the hydrogen bond between Tyr14 and the substrate carbonyl

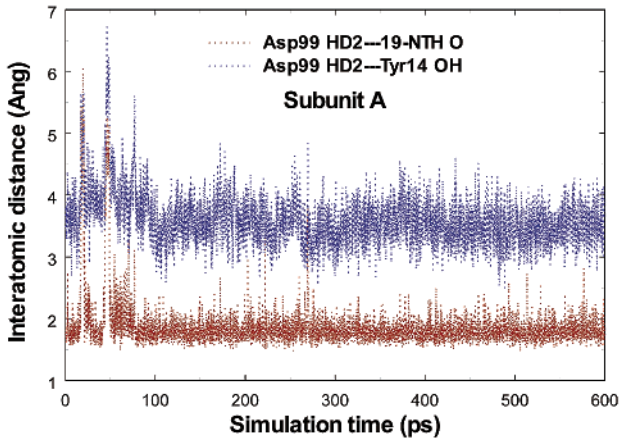

(a)

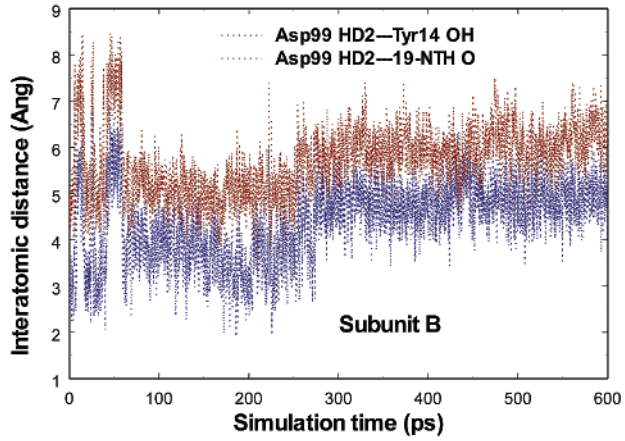

(b)

Figure 5. Comparative view of the time dependence of the interatomic distances between the HD2 atom of Asp99 and substrate carbonyl oxygen and between the HD2 atom of Asp99 and OH atom of Tyr14 in (a) subnuit A and (b) subunit B of the enzyme−19-NTH complex dimer.

group. Interestingly, a few trajectory snapshots showed short hydrogen bond distances of ∼1.5 Å in both monomers. This structural feature may be related to the earlier proposal of the involvement of a strong Tyr14 HH···O$_S$ hydrogen bond.[23] Indeed, the role of Tyr14 in catalysis has been established in mutagenesis studies, which demonstrated that mutation of this residue reduces the catalytic ability of KSI by a factor of $10^{4.7}$.[6a]

To obtain catalytically relevant insights into the active site conformation of the KSI−substrate complex dimer, we measured interatomic distances between Asp99 HD2 and O$_S$ and compared them with the distance between Tyr14 OH and Asp99 HD2. As can be seen in Figure 5a, Asp99 HD2 forms a hydrogen bond with O$_S$ (2.5 Å 98% residence time) in preference to Tyr14 OH in subunit A during the MD simulation. This result indicates that the CH mechanism should be favored over the CD route at least in one subunit of the homodimeric enzyme. Interestingly, Figure 5b shows that Asp99 HD2 is closer to Tyr14 OH than O$_S$ in subunit B for almost the entire simulation. The difference in average values of these interatomic distances is 1.6 Å, suggesting, as required by the CD mechanism, that Asp99 interacts with Tyr14 more favorably than O$_S$. The

(23) Brooks, B.; Phillips, R. S.; Benisek, W. F. *Biochemistry* **1998**, *37*, 9738.

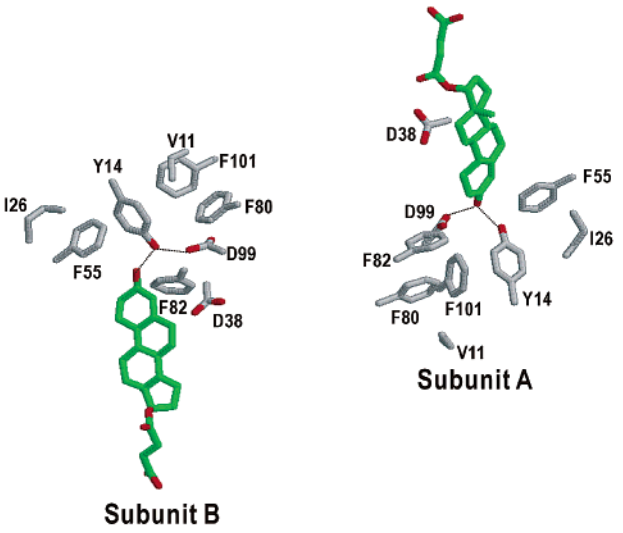

Figure 6. A trajectory snapshot involving the two different catalytic configurations in subunits A and B. Hydrogen atoms are omitted for clarity. The dotted lines indicate the hydrogen bonding interactions.

preference for the CD mechanism in subunit B was further supported by the relative stability of the Tyr14 HH···O_S hydrogen bond compared to that in subunit A (see Figure 4). Indeed, the strengthening of this hydrogen bond interaction, due to the formation of the catalytic diad, has been regarded as an important structural aspect of CD mechanism.[9]

Shown in Figure 6 is a set of snapshots involving the catalytic configurations of subunit A and subunit B in the enzyme−19-NTH complex dimer with apolar residues around the reactive site. During the entire course of the simulation, the carboxylate group of 19-NTH interacts with solvent molecules at a distance of about 17 Å from the key hydrogen bonds in the active site. Note that the key hydrogen bonding groups (Asp 99 and Tyr 14) are surrounded with apolar groups including four phenylalanine residues, indicating the importance of hydrophobic interactions in forming the reactive complex. From Figure 6, it is clear that subunit B has its catalytic groups arrayed in a manner consistent with the CD mechanism of Scheme 1, while subunit A adopts a geometry consistent with the CH mechanism. Thus, the current MD simulation study supports both possibilities, providing evidence for the simultaneous operation of two competing catalytic mechanisms in a dimeric enzyme. However, this is purely structural evidence, and in order for both mechanisms to be relevant, the energetics of these two reactions need to be nearly identical (see section 3.3 for further details). Moreover, because of the differences observed in the NMR and X-ray structures, we decided to complete one more MD simulation on the X-ray structure as a point of comparison to the MD simulation based on the NMR structure.

3.2. MD Simulation of KSI Dimer in Complex with EQU. The root-mean-square deviation from the X-ray structure ($rmsd_{X-ray}$) of all heavy atoms versus the simulation time is displayed in Figure 7. The overall rmsd remains 1−1.5 Å for the entire simulation, implying a sustained stability of the complex dimer. Like the KSI−19-NTH system, the rmsd of subunit A is found to be larger than that of subunit B for most of the simulation time.

To identify stable hydrogen bonding interactions between the intermediate analogue and the active site residues, we measured the interatomic distance between the HD2 atom of Asp99 and

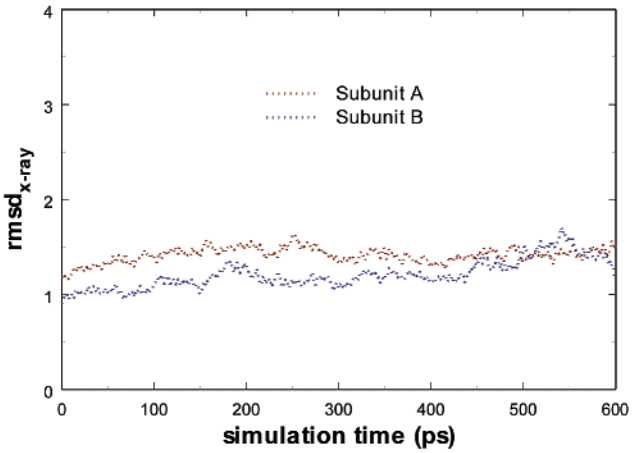

Figure 7. Time dependence of the root-mean-square deviation of each monomer from the crystal structure of the KSI−EQU complex.

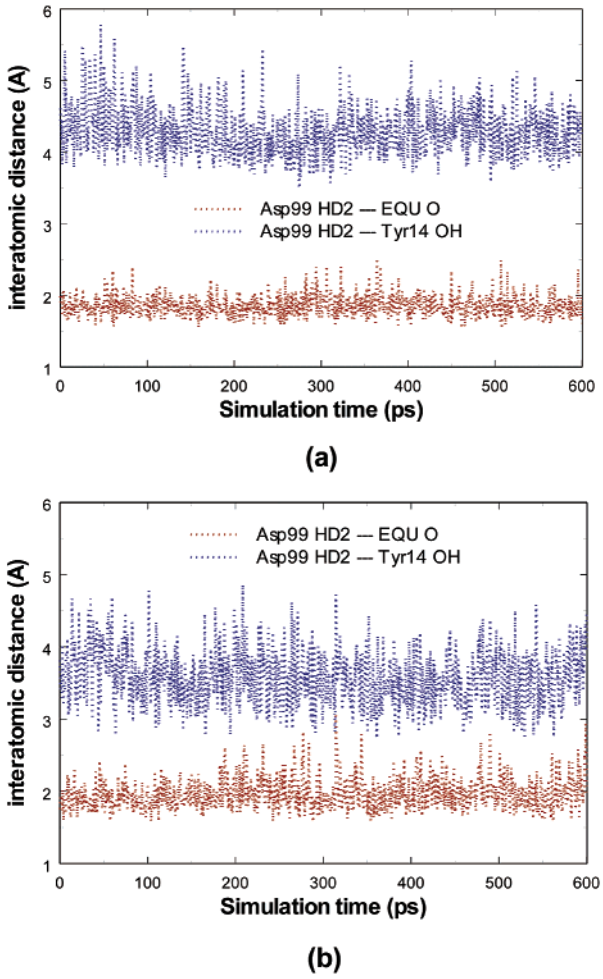

Figure 8. Comparative view of the time evolution of the interatomic distances between the HD2 atom of Asp99 and phenolic oxygen of EQU and between the HD2 atom of Asp99 and the OH atom of Tyr14 in (a) subunit A and (b) subunit B of the enzyme−EQU complex.

the OH atom of Tyr14, as well as that between Asp99 HD2 and the phenolic oxygen of equilenin (EQU O). As can be seen from Figure 8, the hydrogen bond between HD2 and the EQU O is present throughout the simulation in both monomers of the KSI−EQU complex, while the HD2···OH distance is greater than 3 Å for nearly the entire course of the simulation. Thus, the analysis of the MD trajectory for the KSI−EQU system

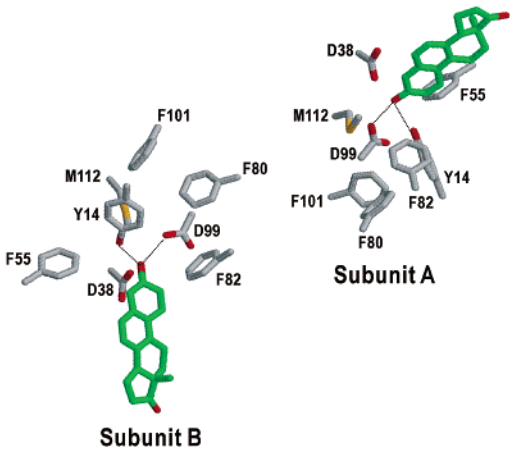

Figure 9. A typical MD trajectory snapshot in which both Tyr14 and Asp99 form a hydrogen bond with the intermediate phenolic oxygen. Hydrogen atoms are omitted for clarity. The dotted lines indicate the hydrogen bonding interactions.

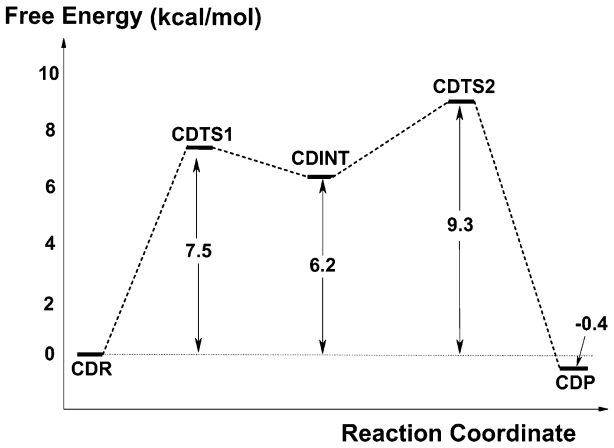

Figure 10. Free energy profile diagram along the intrinsic reaction coordinate of the enzymatic reaction model for the catalytic diad mechanism. For each stationary-state structure, the free energy measured from the reactant complex (**CDR**) is indicated in units of kcal/mol. **CDTS1**, **CDINT**, **CDTS2**, and **CDP** designate the first transition state, reaction intermediate, second transition state, and product complex, respectively.

indicates that the CH mechanism is structurally favored over the CD route.

Figure 9 shows a typical MD snapshot of the hydrogen bonding interactions between the intermediate analogue and the catalytic residues in the KSI−EQU complex. As indicated by Figure 8, both Tyr14 and Asp99 form a hydrogen bond with the phenolic oxygen of EQU in both subunits.

The difference in the hydrogen bonding preferences between the MD simulations based on the NMR and X-ray structures is interesting. There are several competing factors that could explain the observed differences. The substrate analogues (NMR, 19-NTH; X-ray, EQU) are quite different in their hydrogen bonding capabilities. 19-NTH has a carbonyl group that can accept two hydrogen bonds (much like the substrate), while EQU has a hydroxyl group that can accept two hydrogen bonds as well as being able to donate a hydrogen bond. From Figures 6 and 9, we can see how this difference plays a role in defining the active site structure. In Figure 9, D38 (deprotonated) hydrogen bonds to the hydroxyl hydrogen of the substrate and "pulls" this hydrogen atom away from the hydrogen bonding sites occupied by Tyr14 and Asp99, while in the case of 19-NTH this type of interaction is impossible. From the mechanistic proposals (see Schemes 1−3), it is clear that 19-NTH's carbonyl is similar to the actual substrate, while the enolic character of EQU is never formed along the proposed reaction coordinate (indeed, the intermediate is thought to be the enolate). Other differences include the planarity of EQU relative to the actual substrate and to 19-NTH and the charged carboxylate tail of 19-NTH. These differences as well as the differences in the experimental structure determinations (NMR versus X-ray) could explain our observed simulation results. When taken altogether, the simulations and the experimental structures of these substrate and intermediate analogues clearly demonstrate the potential difficulties in defining catalytic roles for specific residues.

3.3. Ab Initio Calculations. To complement the mechanistic insights from the MD simulations, we have also examined the two catalytic possibilities via ab initio calculations on models of the enzyme active site at the MP2/6-31+G**//RHF/6-31G** level of theory. By integrating the structural features obtained from the MD simulations with energetic information obtained from the simplified enzymatic reaction models relevant to the CD and CH mechanisms (see Schemes 1−3), we will address the preferred reaction route for the KSI-catalyzed isomerization reaction.

It should be noted that the hydrophobic environment preventing the approach of solvent molecules shifts the pK_a of Asp 99 abnormally high in the enzymatic active site of KSI (>9) when compared to that in aqueous solution (∼4.4).[7] As in previous theoretical investigations,[12,13] formic acid (pK_a = ∼3.8) was used as a functional mimic of Asp99 in the present study under the assumption that gas-phase formic acid qualitatively reproduces the role of Asp99 in the enzymatic reaction.

3.3.a. Catalytic Diad Mechanism. Figure 10 displays the free energy profile along the reaction path described in Scheme 3A. The first reaction step involves the abstraction of a proton from the α-carbon of the substrate by Asp38, which is accompanied by partial proton transfer from the catalytic diad to the substrate carbonyl oxygen. As a result, a reaction intermediate (**CDINT**) is formed with a free energy of 6.2 kcal/mol above that of the reactant complex (**CDR**), and the activation barrier (**CDTS1**) for the formation of **CDINT** from **CDR** is 7.5 kcal/mol. Next, Asp38 moves the newly acquired proton to the γ-carbon, leading to the formation of the product complex (**CDP**) in which the substrate is transformed into an α, β-unsaturated carbonyl compound. The barrier for the second step (**CDINT → CDTS2)** is found to be 3.1 kcal/mol. Thus, the overall activation energy for the stepwise reaction is the energy difference between the reactant and the second transition state (**CDTS2**), which is 9.3 kcal/mol.

The stationary-state structures located along the reaction path are shown in Figure 11, together with some selected interatomic distances. The KSI reaction starts with the formation of a reactive complex (**CDR**) in which the substrate carbonyl oxygen (O_S) is hydrogen bonded to the phenolic proton (HH) at a distance of 1.82 Å. The phenolic oxygen (OH), in turn, forms a hydrogen bond with the proton (HD2) belonging to the carboxylic acid group of Asp99. In this complex, a carboxylate oxygen (OD) of Asp38 is also hydrogen bound to the substrate α-carbon (C_S) with an associated OD···H_S distance of 2.55 Å. The reaction is initiated by the approach of OD toward H_S, and

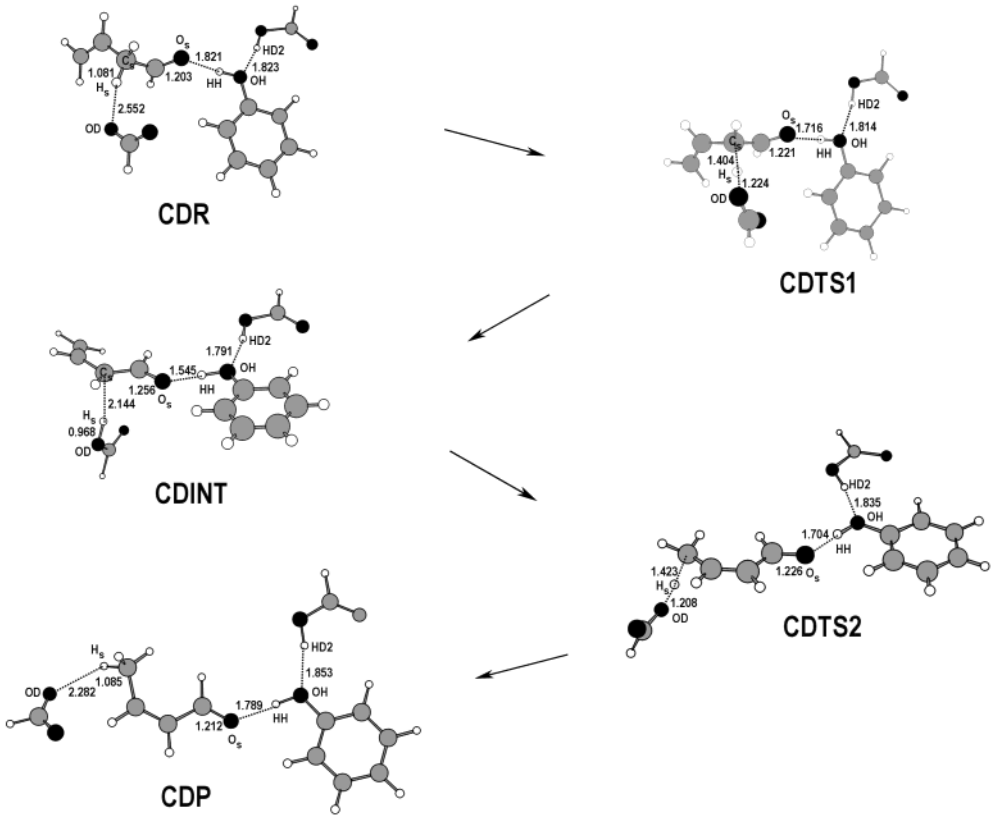

Figure 11. A pictorial description of the enzymatic reaction model for the catalytic diad mechanism. Some selected interatomic distances are given in Å.

when the interatomic separation falls below 1.22 Å, the system reaches the first transition state (**CDTS1**). Concomitant with this change, the O_S···HH hydrogen bond becomes stronger because of the development of negative charge on the O_S atom.

The complete transfer of H_S to OD generates **CDINT**, which corresponds to the dienolate intermediate complexed with the three essential catalytic residues. We find that the hydrogen bond between O_S and the catalytic diad gets even stronger on going from **CDTS1** to **CDINT**, leading to a contraction of the O_S···HH distance to 1.54 Å. In this short strong hydrogen bond, the distance between H-donor and H-acceptor is 2.54 Å, which is comparable to the sum of van der Waals radii of two oxygen atoms (2.55 Å).[24] This result supports the possibility that a short strong hydrogen bond (SSHB) could be involved in enzymatic stabilization of the dienolate intermediate, which has been well characterized in a previous ab initio study.[12] Because of the shortening of the OH···HD2 distance, the formation of such an SSHB can be attributed to a reinforcement of the Asp99···Tyr14 interaction via the OH···HD2 hydrogen bond as well as the electronic rearrangement in the substrate during the catalytic cycle, which enhances the negative charge on O_S.

From the **CDINT**, the second reaction step proceeds with the approach of Asp38, in its protonated form, to the γ-carbon of the substrate, which leads to formation of the rate-limiting transition state (**CDTS2**). In contrast to the first reaction step, the interaction between the substrate oxygen and Tyr14 gets weaker on going from **CDINT** to **CDTS2**, because the C═O bond is restored in the substrate, which results in the lengthening of the hydrogen bond in the catalytic diad. Similar structural features for the reketonization step were also observed in the kinetic and mechanistic studies of KSI.[6e,12] In **CDTS2**, the H_S atom is partially transferred to the γ-carbon with an associated distance of 1.42 Å. This high energy structure then decays to form the product complex (**CDP**), in which the model substrate is fully converted from a β,γ-unsaturated carbonyl to an α,β-unsaturated one with a concomitant weakening of the O_S···HH and OH···HD2 hydrogen bonds.

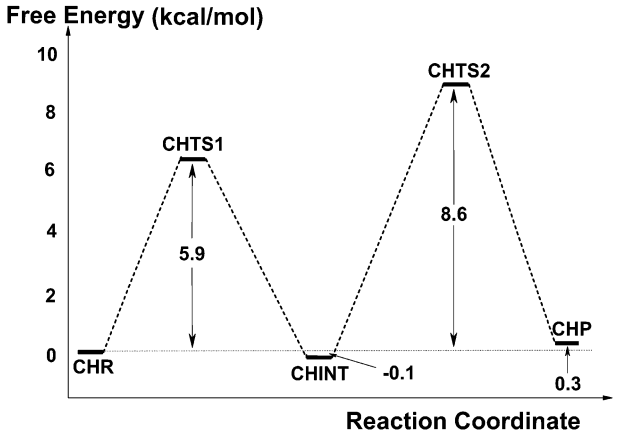

Figure 12. Free energy profile diagram along the intrinsic reaction coordinate of the enzymatic reaction model for the cooperative hydrogen bond mechanism. For each stationary-state structure, the free energy measured from the reactant complex (**CHR**) is indicated in units of kcal/mol. **CHTS1**, **CHINT**, **CHTS2**, and **CHP** designate the first transition state, reaction intermediate, second transition state, and product complex, respectively.

3.3.b. Cooperative Hydrogen Bond Mechanism. Shown in Figure 12 is the free energy profile for the reaction described in Scheme 3B. The first activation barrier is lowered by 1.6 kcal/mol relative to that of the CD mechanism (see Figure 11).

(24) Frey, P. A.; Whitt, S. A.; Tobin, J. B. *Science* **1994**, *264*, 1927.

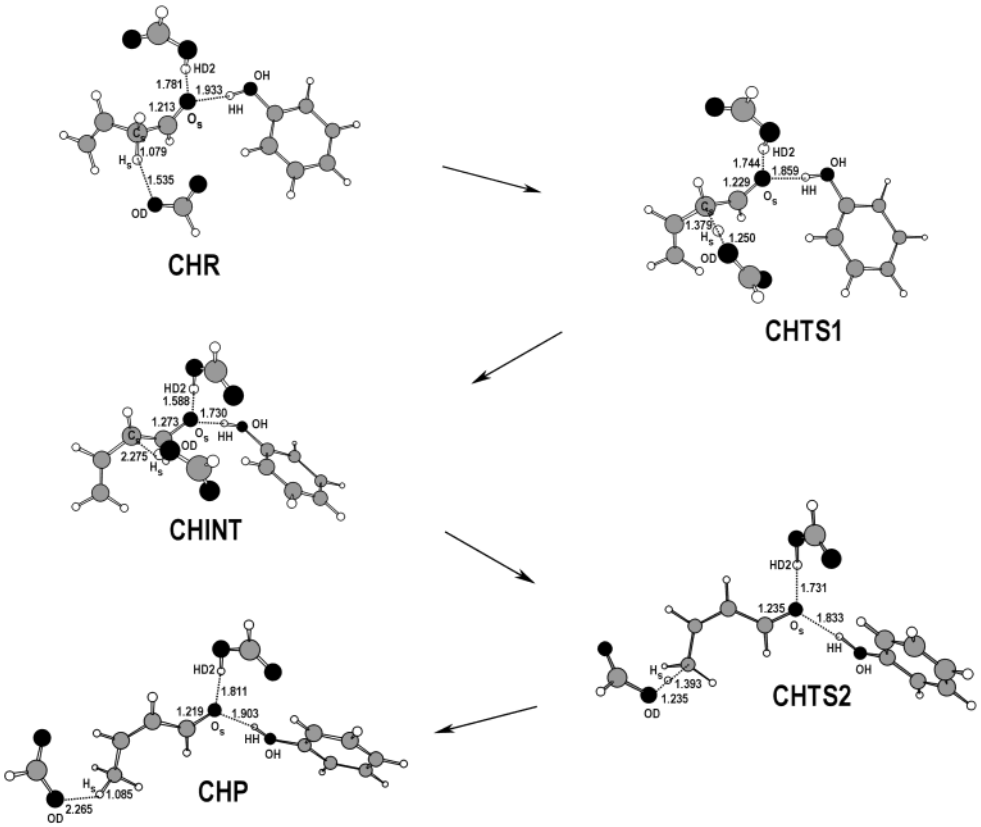

Figure 13. A pictorial description of the enzymatic reaction model for the cooperative hydrogen bond mechanism. Some selected interatomic distances are given in Å.

Most interestingly, the dienolate intermediate is stabilized in this mechanism by 6.3 kcal/mol. Hence, the CH mechanism is more effective in stabilizing the first transition state and the resultant dienolate intermediate. From the reaction intermediate (**CHINT**), however, a free energy barrier of 8.7 kcal/mol must be surmounted to reach the rate-limiting transition state (**CHTS2**) for the reketonization step. Overall, the free energy of activation, which is the energy difference between **CHR** and **CHTS2**, is 8.6 kcal/mol. This is lower than that for the CD mechanism by only 0.7 kcal/mol. This small difference in the free energies of activation prevents us from excluding the possibility of CD mechanism in the catalytic action of KSI.

Figure 13 displays the structures of the reacting system at the energy minima and transition states encountered on the reaction path under investigation. It is interesting to note that, for all five structures, the phenolic group of Tyr14 forms a weaker (via distance considerations) hydrogen bond with the substrate carbonyl oxygen relative to the corresponding structures in the CD mechanism. This is due to the lack of a hydrogen bond interaction between the carboxylic acid group of Asp99 and the phenolic oxygen of Tyr14, which effectively lowers the pK_a of Tyr14.

For the reactive complex, **CHR** in Figure 13, the O_S···HD2 hydrogen bond is shorter (stronger) than the hydrogen bond between HD2 and OH (Tyr14) in **CDR**. As the reaction proceeds, the former interaction undergoes more changes than the latter. For example, the O_S···HD2 hydrogen bond distance is shortened by 0.19 Å on going from **CHR** to **CHINT** relative to a 0.03 Å decrease in the OH···HD2 distance for the first reaction step of the CD mechanism. Thus, it appears that Asp99 interacts more strongly with substrate than with its partner in the catalytic diad (Tyr14).

As indicated above, the most interesting feature of the CH mechanism is the nearly identical stability of the reaction intermediate relative to the reactive complex. This can be attributed to the shortening of the two hydrogen bonds from Tyr14 and Asp99 by 0.20 and 0.19 Å, respectively. In the case of the CD mechanism, the reaction free energy for the formation of the dienolate intermediate (**CDINT**) was predicted to be 6.2 kcal/mol despite a considerable strengthening of the O_S···HH hydrogen bond (0.28 Å). This is 6.3 kcal/mol less stable than **CHINT**, and the free energy of activation is less by 1.6 kcal/mol (**CDTS1** versus **CHTS1**). Thus, clearly multiple hydrogen bond interactions facilitate the formation of the dienolate intermediate in the CH mechanism. Indeed, the importance of lowering the thermodynamic potential for an unstable enolate intermediate has been well appreciated for some examples of enzymatic catalysis.[25]

A common feature of the two catalytic mechanisms is the increase of the hydrogen bonding distance between Tyr14 and Asp99 with the carbonyl oxygen of the substrate in response to the reformation of the C═O bond. In **CHTS2**, the C−O bond has contacted by 70% which directly results in the weakening of the hydrogen bonds between the O_S atom and Tyr14 and Asp99. We note that the lengthening of the O_S···HH hydrogen bond on going from the reaction intermediate (**CHINT**) to the second transition state (**CHTS2**) is 0.06 Å less than that observed in the CD route. This implies that the lack of a direct interaction between Asp99 and Tyr14 leads to a decrease in

(25) Guthrie, J. P.; Kluger, R. *J. Am. Chem. Soc.* **1993**, *115*, 11569.

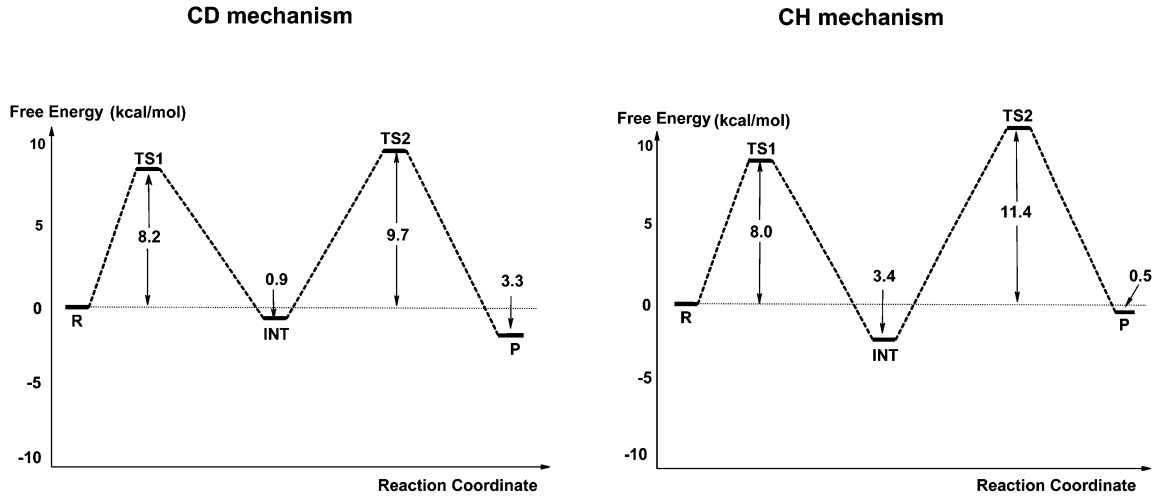

Figure 14. Comparative view of the AM1 free energy profiles associated with modified enzymatic reaction models for CD and CH mechanisms.

Table 1. Relative Contribution of Various Energetic Factors to the Changes in Free Energy for the Catalytic Diad and Cooperative Hydrogen Bond Mechanisms[a]

energy minima and transition states	ΔE_{elec}	$\Delta H'$	$-T\Delta S$	$\Delta G°$
	catalytic diad mechanism			
CDR	0	0	0	0
CDTS1	9.6	−4.0	1.9	7.5
CDINT	6.2	−1.4	1.4	6.2
CDTS2	14.3	−4.2	−0.8	9.3
CDP	1.9	−0.1	−2.2	−0.4
	cooperative hydrogen bond mechanism			
CHR	0	0	0	0
CHTS1	8.1	−4.0	1.8	5.9
CHINT	−0.4	−0.6	0.9	−0.1
CHTS2	12.0	−4.2	0.8	8.6
CHP	2.1	−0.2	−1.6	0.3

[a] Relative free energies ($\Delta G°$) for structures involved in the two reaction paths are calculated by using eq 1. All energies are given in kcal/mol.

the contribution of the latter to enzymatic catalysis. However, the $O_S\cdots$HD2 hydrogen bond, which increases 0.14 Å, clearly is compensating for the reduced catalytic assistance afforded by Tyr14 due to the rupture of the catalytic diad.

3.3.c. Various Energetic Contributions and Their Relevance to Enzymatic Catalysis. Previous theoretical studies of KSI were based on the calculation of the electronic energy profile along the IRC.[12,13] However, it is well-known that entropic effects arising from the thermal nuclear motions transverse to the IRC, including the zero-point vibrational motions, are important in determining the reactivity of weakly bonded complexes.[26] We therefore computed the various thermodynamic quantities at 25 °C and 1 atm by using the usual statistical mechanical expressions.[27] Vibrational frequencies of the complexes required for the calculations were evaluated at the RHF/6-31G** level of theory. Table 1 lists the relative contributions of various energetic factors to the free energies along the reaction profiles.

We note that in both cases the major contribution to the free energy of activation ($\Delta G^{\ddagger}$) comes from the activation enthalpy ($\Delta H^{\ddagger}$) rather than the activation entropy term ($-T\Delta S^{\ddagger}$). Nonetheless, entropic contributions play an important role. Although the enthalpy of activation for the CH mechanism is 2.4 kcal/mol lower than that for the CD counterpart, the difference in free energies of activation is less than 1 kcal/mol when the entropy effect is considered. Thus, we conclude that the direct interaction of Asp99 with substrate is more effective in lowering $\Delta H^{\ddagger}$, while the CD mechanism has the advantage of lowering the kinetic barrier by reducing the entropic penalty for the formation of the rate-limiting transition state.

To obtain further computational evidence for the plausibility of the two competing catalytic pathways, we have also determined the free energy profiles with the AM1 Hamiltonian.[28] These semiempirical calculations were carried out on the modified model system consisting of acetate, acetic acid, phenol, and the entire substrate (anrost-5-ene-3,17-dione), and the results are summarized in Figure 14. It is predicted that the CD mechanism would be kinetically more favorable with a $\Delta\Delta G^{\ddagger}$ of only 1.7 kcal/mol. The error bars associated with the semiempirical calculations is on the order of ±5 kcal/mol; hence, the AM1 results are consistent with the MD simulations of the KSI−19-NTH complex dimer and the ab initio calculations (here, the error bars are significantly less on the order of ±2 kcal/mol), in supporting both mechanistic possibilities. It is noteworthy (but not unexpected) that our AM1 calculations overestimate the stability of the enolate intermediate in both CD and CH mechanisms when compared with the ab initio results (see Figures 10 and 12). A similar trend was also observed in modeling the reaction intermediate of citrate synthase, in which the AM1 energy of the enolate intermediate was predicted to be 5.7−9.5 kcal/mol lower than ab initio results, depending on the details of calculations.[29]

Consistent with previous ab initio free energy profiles, AM1 calculations predict that, in the presence of the electrophilic catalytic groups (Y14 and D99), the formation of the dienolate intermediate should be thermodynamically favorable. Indeed, it is known that enzymes catalyzing a proton abstraction reaction from carbon acids are able to resolve the thermodynamic

(26) (a) Pross, A. *Theoretical and Physical Principles of Organic Reactivity*; Wiely: New York, 1995; pp 130−136. (b) Hobza, P.; Zahradnik, R. *Top. Curr. Chem.* **1980**, *93*, 53.
(27) McQuarrie, D. A. *Statistical Mechanics*; Harper & Row: New York, 1976; pp 35−50.
(28) (a) Dewar, M. J. S.; Thiel, W. *J. Am. Chem. Soc.* **1977**, *99*, 4899. (b) Dewar, M. J. S.; Zoebisch, E. G.; Healy, E. A.; Stewart, J. J. P. *J. Am. Chem. Soc.* **1985**, *107*, 3902.
(29) Mulholland, A. J.; Richards, W. G. *J. Phys. Chem. B* **1998**, *102*, 6635−6646.

problem of stabilizing the enolate intermediate as well as the kinetic problem of lowering the free energy of activation. In the case of the KSI-catalyzed isomerization reaction of a ketosteroid substrate, kinetic studies indicate that the free energy of the reaction intermediate would be comparable to those of the enzyme−substrate and enzyme−product complexes.[30]

There has been a long debate regarding the source of catalytic power for highly efficient enzymatic reactions. It has been proposed, for example, that enzymatic rate enhancement can be attributed to the formation of LBHBs between substrate and enzyme in transition states or intermediates, and this hypothesis was supported by the matching of pK_a values between donor and acceptor groups.[31] On the other hand, a combination of multiple hydrogen bond interactions with individually modest contributions was also found to be a catalytic strategy for highly proficient enzymes.[32] On the basis of the similarity in $\Delta G^{\ddagger}$ values for the CD and CH mechanisms, we suggest that both kinds of interactions play a significant catalytic role in the action of KSI with each having its own ability to reduce $\Delta G^{\ddagger}$.

4. Conclusions

We have investigated the plausibility of two catalytic mechanisms (catalytic diad (CD, Scheme 3A) and cooperative hydrogen (CH, Scheme 3B) bond mechanisms) for the KSI-assisted isomerization reaction on the basis of the MD simulation of the enzyme in complex with a substrate and an intermediate analogue and quantum chemical calculations on relevant enzymatic reaction models. We found from an MD simulation of the KSI−19-NTH (substrate analogue) complex dimer that the hydrogen bond between the substrate carbonyl group and the side chain of Tyr14 was established in both monomers of the enzyme−substrate complex dimer. In most of the trajectory snapshots, the side chain of Asp99 donates an additional hydrogen bond to the substrate carbonyl oxygen in one subunit, consistent with the CH mechanism. In the other subunit, however, the carboxylic acid group of Asp99 is closer to the phenolic oxygen of Tyr14 than the substrate carbonyl oxygen over the entire course of simulation, suggesting the CD route. On the other hand, a catalytic configuration supporting the CH mechanism was only found in the MD simulation of the KSI−EQU (intermediate analogue) complex dimer. Furthermore, quantum chemical calculations on model systems indicated that the CH mechanism is thermodynamically favored. Overall, the computational results favor the CH mechanism. However, the CD mechanism could not be excluded unambiguously because of the occurrence of the catalytic diad configuration in one of the subunits in the MD simulation of the KSI−19-NTH complex and the observation that the intrinsic activation parameters for the CH and CD mechanisms are within the error bars of the quantum chemical calculations.

The KSI−19-NTH system reflects the substrate bound form of the enzyme, while the KSI−EQU reflects the intermediate bound form (the proposed intermediate is the enolate and not the enol as seen in EQU). Thus, one interpretation of the data is substrate can bind as proposed by the CH or CD mechanisms, while once the enolate intermediate is formed the need for extra stabilization of the charge shifts the equilibrium in favor of the hydrogen bonding pattern associated with the CH mechanism. The KSI−EQU structure is an intermediate mimetic, but since it is present as the enol and not the enolate, the hydrogen bonding pattern is likely to be different; whether this would shift the equilibrium toward the CD hydrogen bonding pattern is unknown. Testing this hypothesis, as well as others, will be the focus of future research.

Acknowledgment. We thank the NIH (GM 44974) for generous support of this work.

JA0208097

(30) Hawkinson, D. C.; Eames, T. C. M.; Pollack, R. M. *Biochemistry* **1991**, *30*, 10849.
(31) (a) Cleland, W. W.; Kreevoy, M. M. *Science* **1994**, *264*, 1887. (b) Cleland, W. W.; Frey, P. A.; Gerlt, J. A. *J. Biol. Chem.* **1998**, *273*, 25529.
(32) (a) Jencks, W. P. *Adv. Enzymol. Relat. Areas Mol. Biol.* **1975**, *43*, 219. (b) Fierke, C. A.; Jencks, W. P. *J. Biol. Chem.* **1986**, *261*, 7603. (c) First, E. A.; Fersht, A. R. *Biochemistry* **1995**, *34*, 5030. (d) Shan, S.; Herschlag, D. *J. Am. Chem. Soc.* **1996**, *118*, 5515.